JOURNAL OF MATERIALS SCIENCE 27 (1992) 1016–1022

Microstructural developments in Mg–Ti–PSZ systems

P. R. KRISHNAMOORTHY, PARVATI RAMASWAMY, B. H. NARAYANA
Materials Technology Division, Central Power Research Institute, P.B. 9401, Bangalore 560 094, India

The microstructure of titania-added Mg–partially-stabilized zirconia (PSZ) is dramatically influenced by thermal treatments. Effects of various sintering, heat-treatment and thermal shock cycling parameters on the microstructure of the Mg–Ti–PSZ system are described. Conditions favourable for the growth of needle-like Ti-rich reinforcements in highly thermal-shock-resistant Mg–Ti–PSZ ceramics are identified. TiO_2 seems to play a catalytic role in the formation of Zr-rich networks during high-temperature (1700 °C) sintering of the Mg–Ti–PSZ system, quite similar to those found in Mg–PSZ, heat-treated above 1300 °C.

1. Introduction

Among the various commonly known partially stabilized zirconia (PSZ), Mg–PSZ has attracted wide attention because of its tendency for microstructural adaptations, making it suitable for a variety of engineering applications. The sub-eutectoid decomposition of Mg–PSZ in the temperature range 800–1100 °C, apart from imparting improvement in the thermomechanical properties [1, 2], has resulted in unusual microstructures. Degradation of material properties through "destabilization" occurring during the sub-eutectoid decomposition has long been a cause for concern in applications. Hannink and Garvie [1] report the occurrence of metastable intermediate compounds $Mg_2Zr_5O_{12}$ (δ-phase) in Mg–PSZ, along with the development of fine tetragonal, monoclinic zirconia precipitates and MgO-rich regions responsible for enhanced thermal shock resistance. Farmer *et al.* [2] describe the microstructure as consisting of decomposition products, mainly monoclinic ZrO_2, forming a boundary phase around the cubic grains and the δ-phase precipitates contained in the c-ZrO_2 matrix. Heat treating Mg–PSZ above the eutectoid temperature (1300–1450 °C) has, on the other hand, resulted in microstructures consisting of many different precipitate and phase formation sequences [3]. These consist of tetragonal and monoclinic zirconia precipitates, invariably in lenticular shape; large, isolated or randomly oriented network shape; and/or secondary/intermediate precipitate growth.

Various sintering and heat-treatment schedules have been correlated with thermomechanical properties by several workers to make Mg–PSZ suitable for industrial and engineering applications [4, 5].

An entirely different mechanism of destabilization and improvement in thermal-shock resistance has been reported [6, 7] employing TiO_2 additions to Mg–PSZ. The improved thermal-shock resistance is attributed to the formation of needle-like Ti-rich whiskers in Mg–Ti–PSZ ceramics during the up and down thermal shock cycling between 1150 and 25 °C (RT). The effects of heat treatment on the thermomechanical properties of these compositions have been reported elsewhere [8]. The microstructural features and peculiarities arising out of various sintering, heat-treatment and thermal shock-cycling schedules in the Mg–Ti–PSZ and Mg–PSZ systems are described.

2. Experimental procedure

2.1. Sample preparation

Mg–PSZ material (M_{10}) was prepared by wet ball milling ZrO_2 (Indian Rare Earths Ltd, Kerala; 97.5% purity; average particle size, 2–3 μm) and 10 mol % MgO (Loba-Chemie Indo Austranal Co., Bombay; 98.5% purity; average particle size, 1–2 μm) in agate media. This was followed by oven drying, granulating with PVA and uniaxial pressing at 400 kg cm^{-2} to form rectangular bars of 50 × 25 × 8 mm. Addition of 4 and 6 mol % TiO_2 (FERAK Laborat GMBH, Berlin; 99.9% purity; average particle size, 1–2 μm) to the M_{10} composition followed by the same processing techniques made the compositions in the Mg–Ti–PSZ system ($M_{10}T_4$ and $M_{10}T_6$). Two batches of these compositions were sintered at 1500 and 1700 °C, respectively, in an electrical furnace for 4 h. The furnace was shut off at the end of 4 h soaking at the sintering temperature.

2.2. Thermal shock testing

The up and down thermal-shock test consisted of introducing the sample into an electrical furnace maintained at 1150 °C, holding for 1 h and quenching in water at 25 °C (RT).

0022–2461

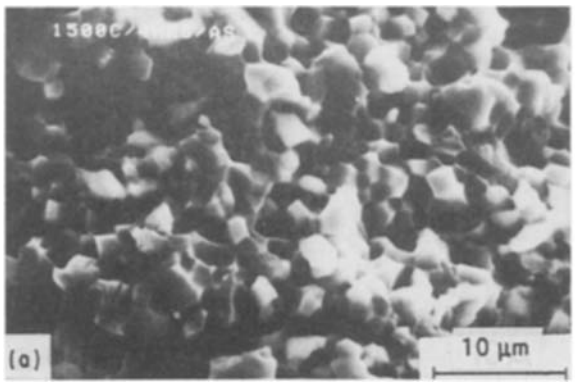

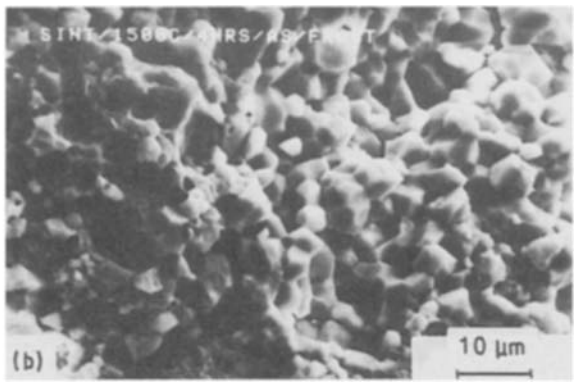

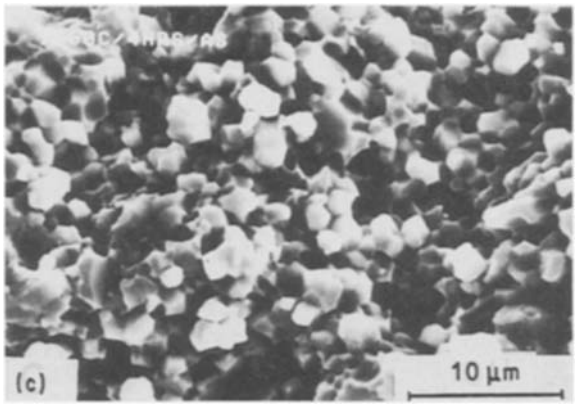

Figure 1 SEM fractographs of samples sintered at 1500 °C for 4 h: (a) M_{10}; (b) $M_{10}T_4$; (c) $M_{10}T_6$.

2.3. Microscopy

Microstructural and microchemical analyses were carried out by scanning electron microscope (SEM) and energy dispersive X-ray analysis (EDXA).

3. Results and discussion

3.1. Specimens sintered at 1500 °C

3.1.1. SEM fractography

Fractographs of M_{10}, $M_{10}T_4$ and $M_{10}T_6$ specimens sintered at 1500 °C for 4 h are shown in Fig. 1. Uniformly distributed polyhedral grains form the salient features of both Mg–PSZ and Mg–Ti–PSZ specimens. While the grain size of the M_{10} composition (Fig. 1a) is about 3–6 μm, those of $M_{10}T_4$ and $M_{10}T_6$ are about 2–3 μm (Fig. 1b, c). Some of the pores with regular geometrical shapes can be attributed to grain pull-out in the fractured specimen. Furthermore, uniform distribution of pores in an otherwise featureless microstructure is also seen. Titania, although a sintering aid, appears to act as a grain growth inhibitor in Mg–PSZ, as seen in these micrographs.

3.1.2. Thermally quenched specimens—SEM fractography

Fractographs of M_{10} failed after 42 thermal-shock cycles, and $M_{10}T_4$ and $M_{10}T_6$ fractured (not failed) after 50 thermal-shock cycles, are presented in Fig. 2. Thermal shock treatment (M_{10}, 42 cycles) seems to result in the development of inter- and intragranular crack networks. Apart from this, the treatment does

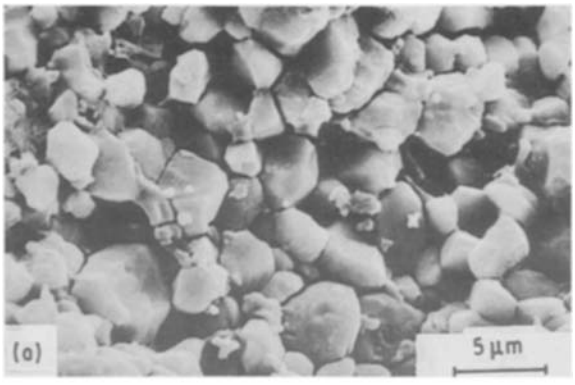

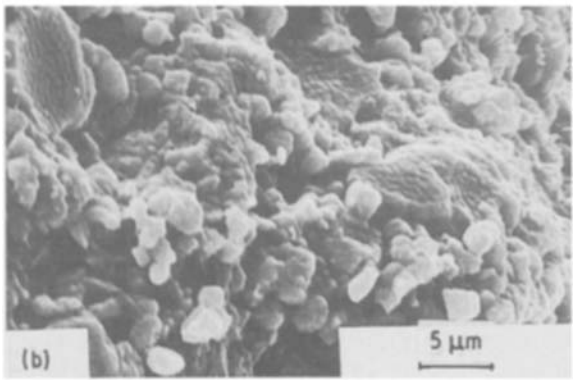

Figure 2 SEM fractographs of sintered samples after thermal quench cycles between 1150 °C and water at 25 °C (RT). (a) M_{10} (42 cycles—F); (b) $M_{10}T_4$ (50 cycles—NF); (c) $M_{10}T_6$ (50 cycles–NF); F, failed; NF, not failed.

not appear to have brought about any significant microstructural changes in the M_{10} composition (Fig. 2a). In contrast, the $M_{10}T_4$ (Fig. 2b) and $M_{10}T_6$ (Fig. 2c) thermal-shock-treated samples reveal interesting microstructural changes compared to the as-sintered specimens. Partial spherodization of grains and initiation of fibrous features on the grain surfaces are evident in the $M_{10}T_4$ fractographs. A much higher degree of spherodization of grains and clusters of fibrous networks, apart from needle-like whiskers, are clearly seen in the $M_{10}T_6$ fractograph. Fig. 2b ($M_{10}T_4$) represents the intermediate stage of development of microstructural features in the Mg–Ti–PSZ system.

3.1.3. Thermally quenched specimens—microchemical analysis

Hannink [5] and others [2, 9] have reported the occurrence of decomposition of Mg–PSZ containing 8.1 and higher mol % MgO when heat-treated (aged and furnace cooled) in the sub-eutectoid temperature regime around 1100 °C. They report the occurrence of the classical form (m-ZrO_2) of decomposition within the grain boundary regions around the c-ZrO_2 matrix seen in optical micrographs. TEM analyses of the grain boundary precipitate are reported to consist of the following:

(i) Polygonized regions of m-ZrO_2 (~ 2.5 μm) with m-subgrains (~ 0.1 μm);
(ii) MgO pipes 0.1 μm thick and 1 μm long, forming the boundaries between the polygonized m-regions;
(iii) Microcrack networks due to thermal expansion differences between various m-ZrO_2 orientations and extensive crack–MgO pipe interaction.

Spherodization of grains was not observed in any of the above cases. Spherodization, interwoven networks of fibrous features and growth of needle-like features under thermal shock are peculiar to Mg–Ti–PSZ compositions, and are not found in the Mg–PSZ system, pointing to the presence of TiO_2 as being responsible for these unusual features. However, in order to understand if these needle-like features and networks are similar to the sub-eutectoid decomposition products [2, 5, 9], both as-sintered and thermally shocked specimens were further studied using qualitative microchemical analysis techniques (EDXA) (Figs 3 and 4). From Fig. 3a, it is clear that as-sintered grains of M_{10} consist of Zr and small amounts of Mg, while those of $M_{10}T_4$ (Fig. 3b) and $M_{10}T_6$ (Fig. 3c) consist of Zr and small amounts of Ti and Mg. The microstructure and microchemical analysis of thermally shocked $M_{10}T_4$ and $M_{10}T_6$ warrant more detailed discussion.

From Fig. 2b, it is seen that $M_{10}T_4$, after having undergone 50 thermal quench cycles, consists of (a) partially spherodized and smooth grains; and (b) partially spherodized grains with fibrous features on the surface. From the EDX analysis of $M_{10}T_4$ after 50 thermal-quench cycles (Fig. 4a), it is seen that the smooth grains consist of Zr and small amounts of Mg

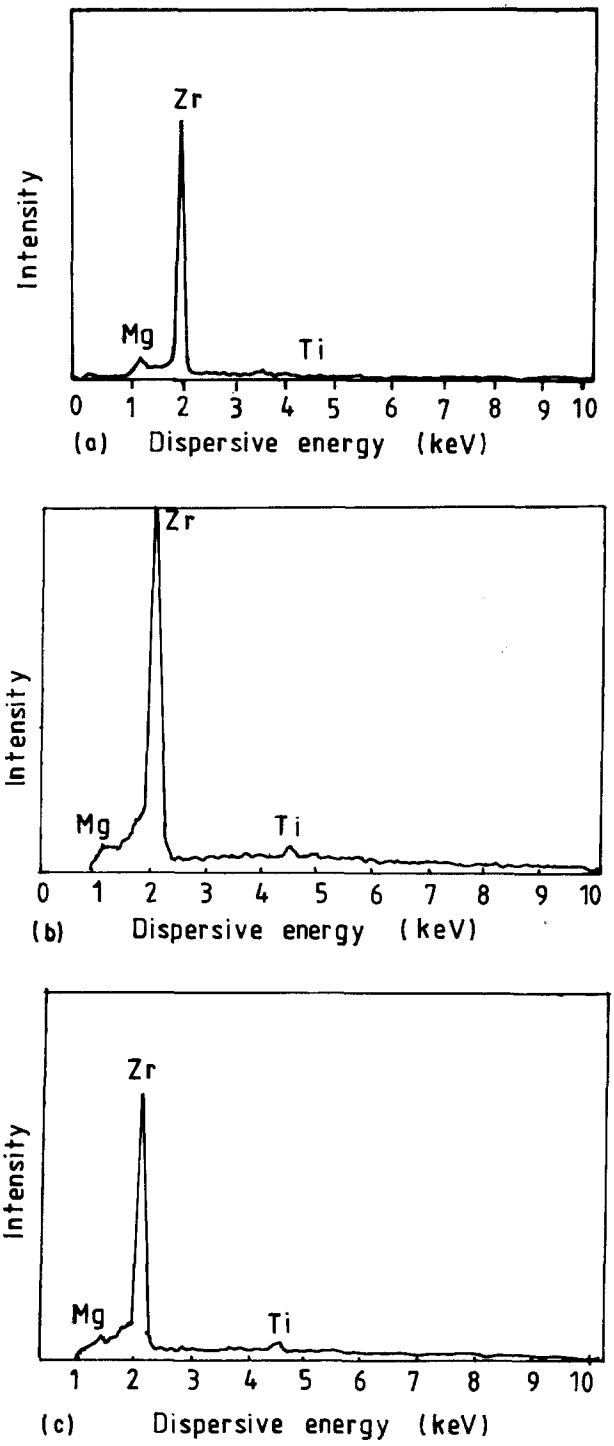

Figure 3 EDX analysis of grains in as sintered samples at 1500 °C for 4 h: (a) M_{10}; (b) $M_{10}T_4$; (c) $M_{10}T_6$.

and Ti, similar to those of as-sintered grains (Fig. 3b). However, the microchemical area analysis of the grains with fibrous features (Fig. 4b) shows a different chemical constitution from that of smooth grains. These grains consist of predominant phases of Ti and Zr, and a small amount of Mg. The fractograph of $M_{10}T_6$ after undergoing 50 thermal shock cycles, shown in Fig. 2c, reveals the following features: (i) spherodized and smooth grains with chemical constitution similar to as sintered grains; (ii) spherodized grains with fibrous features on the surface consisting of Ti- and Zr-rich phases with a small amount of Mg; (iii) clusters of fibrous features forming a network and needle-like features ~ 10–12 μm long and 1–2 μm thick.

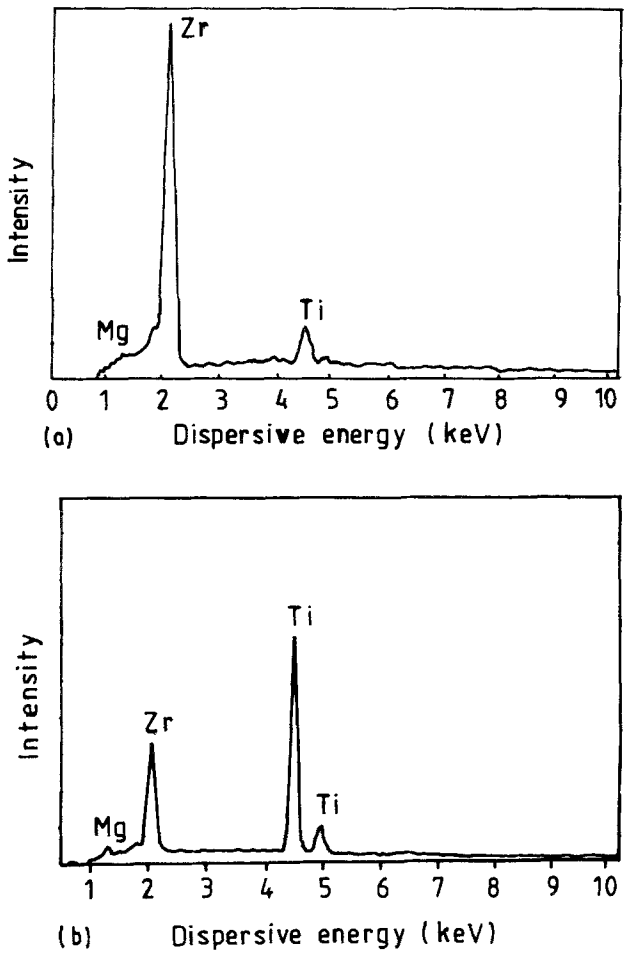

Figure 4 EDX analysis of grains in $M_{10}T_4$ samples after thermal quench cycles (50 times between 1150 °C and water at 25 °C). (a) Normal grains; (b) grains with fibrous features.

The network and needle-like features, however, consist of an entirely different chemical composition. These features consist of a phase rich in Ti, with small amounts of Zr and Mg (Fig. 5). Absence of visible MgO-rich regions in both SEM micrographs and microchemical EDX area analyses rules out the possibility of the growth of MgO-rich pipe-like structures, beyond 1 μm or so, in the Mg–Ti–PSZ system during thermal-shock treatment.

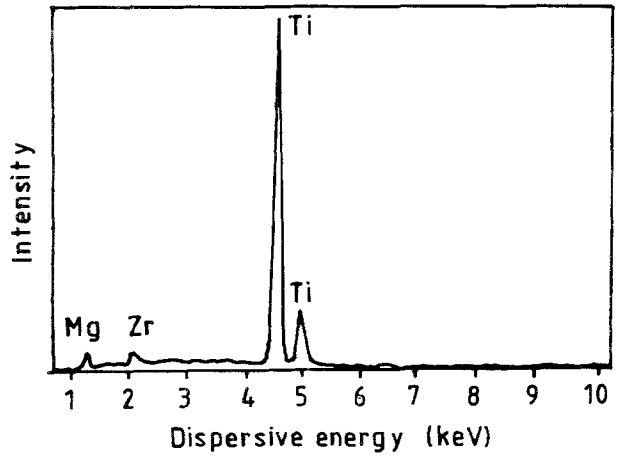

Figure 5 EDX analysis of needle-network in $M_{10}T_6$ samples after thermal-quench cycles (50 times between 1150 °C and water at 25 °C).

3.1.4. Ti-rich reinforcements—conditions for growth

Our attention is now focused on the conditions of formation of Ti-rich interwoven network of fibrous and needle-like features which act as reinforcements [6] in the Mg–Ti–PSZ ceramic system. In order to understand the significant effects, if any, of temperature on the formation of these features, $M_{10}T_6$ was thermally shocked and cycled between 1000 °C and water at 25 °C while maintaining the hold time of 1 h in between the cycles, similar to the previous experiments. The tests were stopped at the end of 50 cycles. Based on reports of tests conducted as laboratory experiments [11] it is understood that such thermal-shock-cycling tests are generally stopped after about 25 cycles, to classify a material as possessing good resistance to thermal shock. Further, the microstructural development in PSZ systems similar to ours is known to occur by ageing or other heat treatment within 8 or 10 h [1]. The thermal-shock treatment in the present work has been conducted for 50 long (1 h) cycles to ensure complete development of microstructural features. Fig. 6 shows the fractograph of an $M_{10}T_6$ specimen after having undergone 50 thermal quench cycles between 1000 °C and water at 25 °C (RT). The absence of any visible changes from that of an as-sintered microstructure (Fig. 1c) indicates that a temperature of 1000 °C is not high enough to bring about the spherodization of the grains or formation of needle network features in this system while retaining the polyhedral grain shape.

Figure 7 shows a fractograph of $M_{10}T_6$ heat-treated (furnace hold 50 h and furnace cool) at 1150 °C for 50 h. A similar microstructure was observed when the $M_{10}T_6$ specimen was held at 1150 °C for 50 h and quenched in water at 25 °C (figure not given). Spherodization in the presence of only isolated network features and needles similar to those seen in Fig. 2c (50 1 h thermal quench cycles 1150–25 °C) suggests the necessity of thermal quenching for the growth of Ti-rich reinforcements associated with a high-temperature differential of > 1000 °C, perhaps 1100 °C. Thermal quench cycling between 1200 °C and water has also resulted in the formation of similar needle-like features.

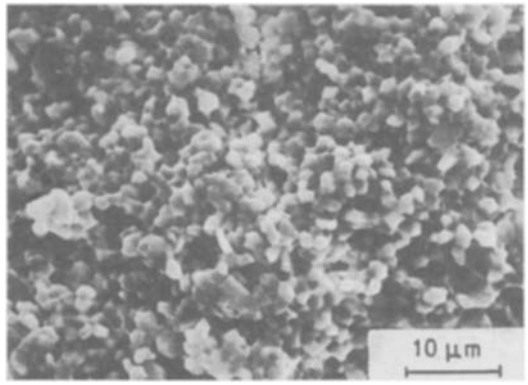

Figure 6 SEM micrograph of fractured $M_{10}T_6$ surface after 50 thermal-quench cycles between 1000 °C and water at 25 °C.

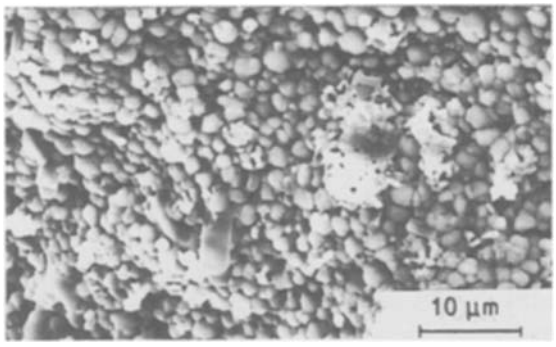

Figure 7 SEM micrograph of fractured $M_{10}T_6$ surface after 50 h of continuous hold at 1150 °C and furnace cooling (heat treatment).

Fig. 8 shows the fractograph of an $M_{10}T_6$ specimen after having undergone 23 thermal-quench cycles between 1150 and 25 °C (RT). Initiation of network feature formation is seen. Such initiation was absent in samples having undergone about ten such thermal-quench cycles (not shown). This indicates the possibility of a requirement of a minimum number of quench cycles for the growth of network features. This also suggests that these features are fully developed when the specimens are thermally quenched between 1150 and 25 °C, 25 or more times. It may also be noted that these needle-network features are formed when the specimens are quenched from 1150 °C to either water or air at about 25 °C (RT).

Experiments with $M_{10}T_4$ and $M_{10}T_6$ specimens employing short-duration thermal quench cycles (1150 °C, 5 min and water quench at 25 °C) did not reveal any fibrous features or whisker formations even after 100 short cycles.

Thus the necessary conditions for the formation of Ti-rich reinforcements in the Mg–Ti–PSZ system are derived as (i) a minimum hold temperature (~ 1100 °C); (ii) a minimum hold time at the hold temperature; (iii) quenching between the hold temperature and RT; and (iv) a minimum number of such thermal quenches.

3.2. Specimens sintered at 1700 °C

3.2.1. SEM fractography

Commercially available Mg–PSZ ceramics are normally processed by adopting careful sintering and heat-treatment schedules in order to make the material suitable for a variety of industrial and engineering applications. They are generally sintered and solution treated in the range of 1700–1800 °C followed by ageing either at ~ 1400 or about 1100 °C.

The effect on microstructure of sintering Mg–PSZ (M_{10}) and Mg–Ti–PSZ ($M_{10}T_4$ and $M_{10}T_6$) at 1700 °C is seen in Fig. 9. Polyhedral grains of about 20 μm with uniformly distributed porosity form the salient feature (Fig. 9a) of M_{10} composition. Grain sizes of about 60 μm have been reported [5] for similar compositions sintered at 1750 °C. It is to be noted that our compositions have not been solution annealed at any temperature in order to cater to grain growth or precipitation.

3.2.2. Microchemical analysis of the needle-network

The microstructure of as-sintered fractured specimen M_{10} displaying smooth extended petal-like features is evidence for local plastic flow and the degree of ductile

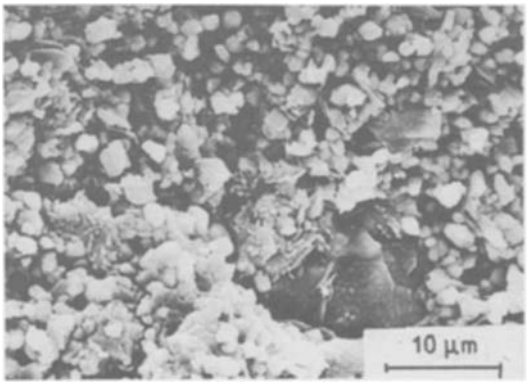

Figure 8 SEM micrograph of fractured $M_{10}T_6$ surface after 23 thermal quench cycles between 1150 °C and water at 25 °C (RT).

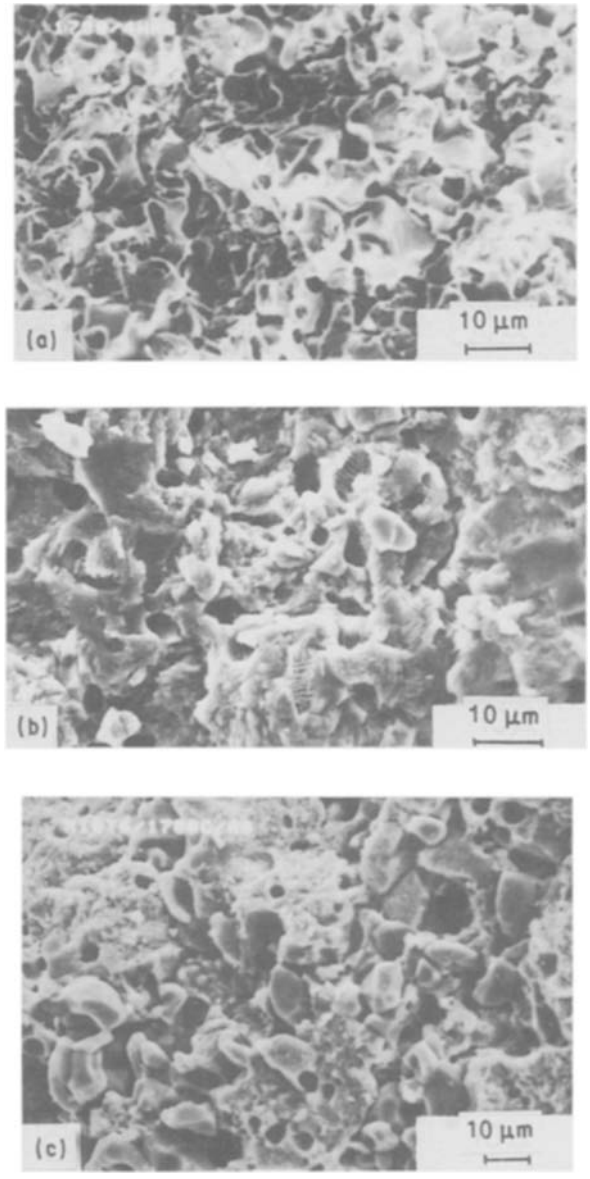

Figure 9 SEM micrograph of samples sintered at 1700 °C for 4 h: (a) M_{10}; (b) $M_{10}T_4$; (c) $M_{10}T_6$.

nature of fracture in the specimen (Fig. 9a). Such features were not observed in the specimens sintered at lower temperatures (compare Fig. 1a). In contrast, the fractographs of $M_{10}T_4$ (Fig. 9b) and $M_{10}T_6$ (Fig. 9c) specimens show more defined polyhedral grain features and also indicate a much lesser degree of ductile fracture. Comparing with the fractographs of these specimens sintered at 1500 °C, we observe a certain extent of smudginess. Detail of this feature at higher magnification is presented in Fig. 10a, where the intergranular cracks are clearly visible. The individual grains or grain clusters are covered with a fabric of needle-networks which are referred to as smudgy features in Fig. 9c. This possibly forms the intergranular precipitate region.

Microchemical area analysis of the network features in Fig. 10a reveal very clearly that the chemical composition of the needle-network phase is very similar to the grains of $M_{10}T_6$ sintered at 1500 °C, i.e. a Zr-rich phase with a small amount of Ti and Mg (Fig. 10b). The Ti-rich phase is seen to be absent in these materials.

Buykx and Swain [12] report the formation of similar microstructural networks or features in aged Mg–PSZ, the temperatures for sintering and ageing being about 1800 and 1320–1400 °C 8 h^{-1}, respectively. These network features consisting of monoclinic precipitates have been attributed to overageing at temperatures above 1300 °C. Taking a clue from this, the formation of a Zr-rich network in $M_{10}T_6$ sintered at 1700 °C may be ascribed to the TiO_2 phase acting as a catalyst in overageing the monoclinic grains or precipitates during the process of sintering itself. The thermomechanical properties and microstructural features of these ceramic compositions will be the subject of future reports.

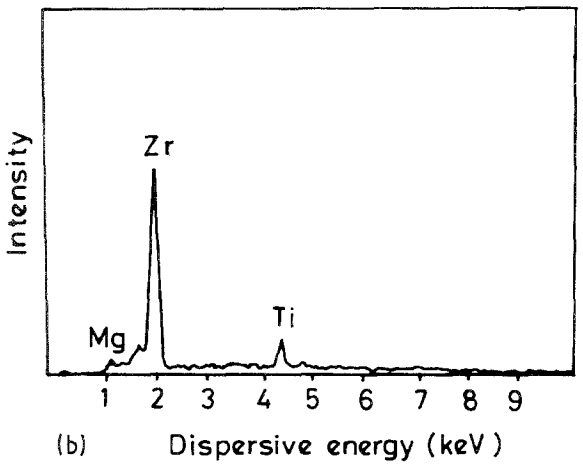

Figure 10 (a) SEM micrograph of $M_{10}T_6$ sintered at 1700 °C, for 4 h showing network features. (b) EDX analysis of the network features shown in (a).

4. Conclusions

The role of TiO_2 in the microstructural development of the Mg–Ti–PSZ system may be summarized as follows.

1. TiO_2 additions generally inhibit grain growth during sintering.
2. The formation of peculiar fibrous features on the sintered ZrO_2 grains either during sintering or during a thermal quench treatment is attributable to the presence of TiO_2 in the system.
3. The Ti-rich fibrous phase with small amount of Zr and Mg on the grains appears to precipitate and grow as separate whisker- or needle-networks in specimens sintered at 1500 °C on thermal quench cycling.
4. Essential conditions for the formation of the Ti-rich whisker-reinforcement phase in specimens sintered at 1500 °C are found to be (i) hold at a temperature of 1100–1150 °C; (ii) hold duration of ~ 1 h in between cycling; (iii) quench between the hold temperature and 25 °C (RT); and (iv) perform a minimum number of thermal quenches.
5. The presence of Ti appears to catalyse the formation of Zr-rich needle-networks while sintering at 1700 °C.

Acknowledgements

The authors thank the management of CPRI for permission to publish this work. Grateful acknowledgements are due to Mr S. Vynatheya for carrying out the experimental work and to M/S Defence Metallurgical Research Laboratory, Hyderabad, India, for conducting the EDX analysis.

References

1. R. H. J. HANNINK and R. C. GARVIE, *J. Mater. Sci.* **17** (1982) 2637.
2. S. C. FARMER, T. E. MITCHELL and A. H. HEUER, in "Diffusional Decomposition of *c*-ZrO_2 in Mg–PSZ", Advances in Ceramics, Vol. 12, Science and Technology of Zirconia II, edited by N. Claussen, M. Rühle and A. H. Heuer, (American Ceramic Society, Columbus, OH, 1983) p. 152.
3. R. R. HUGHAN and R. H. J. HANNINK, *J. Amer. Ceram. Soc.* **69** (1986) 556.
4. R. H. J. HANNINK and M. V. SWAIN, in "Particle Toughening in Partially Stabilized Zirconia, Influence of Thermal History" Materials Science Research, Vol. 20, edited by R. E. Tressler, G. L. Messing, C. G. Pantano and R. E. Newnham (Plenum, New York, 1985) 259.
5. R. H. J. HANNINK, *J. Mater. Sci.* **18** (1983) 457.
6. P. R. KRISHNAMOORTHY, PARVATI RAMASWAMY and B. H. NARAYANA, *Ceram. Int.* **16** (1990) 129.

7 *Idem, Solid State Phenom.* **8, 9** (1989) 501.
8 *Idem, J. Mater. Sci. Lett.* **10** (1991) 464.
9 S. C. FARMER, L. H. SCHOENLEIN and A. H. HEUER, *J. Amer. Ceram. Soc.* **66** (1983) C107.
10 D. L. PORTER and A. H. HEUER, *ibid.* **62** (1979) 298.
11 P. V. ANANTHAPADMANABHAN, S. B. MENON, N. VENKATARAMANI and V. K. ROHATGI, *Ceram. Int.* **12** (1986) 107.
12 W. J. BUYKX and M. V. SWAIN, Advances in Ceramics, Vol. **12**, Science and Technology of Zirconia II, edited by N. Claussen, M. Rühle and A. H. Heuer (American Ceramic Society, Columbus, OH, 1983) p. 518.

Received 25 October 1990
and accepted 25 March 1991